

Highly Efficient Multisubstrate Agricultural Waste-Derived Activated Carbon for Enhanced CO₂ Capture

Mardikios Maja Bade, Amare Aregahegn Dubale,* Dawit Firemichael Bebizuh, and Minaleshewa Atlabachew



Cite This: *ACS Omega* 2022, 7, 18770–18779



Read Online

ACCESS |



Metrics & More

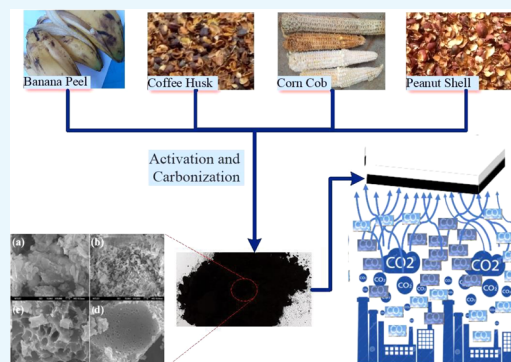


Article Recommendations



Supporting Information

ABSTRACT: Activated carbon (AC) made of single-substrate agricultural wastes is considered to be a suitable raw material for the production of low-cost adsorbents; however, the large-scale application of these materials is highly limited by their low efficiency, seasonal scarcity, poor stability, low surface area, and limited CO₂ adsorption performance. In this study, composite activated carbon (CAC) was prepared via controlled carbonization followed by chemical activation of four wastes (i.e., peanut shell, coffee husk, corn cob, and banana peel) at an appropriate weight ratio. The Na₂CO₃-activated CAC showed a higher surface area and valuable textural properties for CO₂ adsorption as compared with KOH- and NaOH-activated CAC. The CAC production parameters, including impregnation ratio, impregnation time, carbonization temperature, and time, were optimized in detail. The as-prepared CACs were characterized by X-ray diffraction (XRD), scanning electron microscopy (SEM), energy dispersive spectroscopy (EDS), Raman spectroscopy, N₂ adsorption–desorption isotherm, and iodine number analysis. The CAC produced at optimal conditions exhibited the highest CO₂ removal efficiency and adsorption capacity of 96.2% and 8.86 wt %, respectively, compared with the single-biomass-derived activated carbon. The enhanced CO₂ adsorption performance is due to the large surface area, a considerable extent of mesopores, and suitable pore width. The adsorbent in this study reveals a promising strategy for mitigating the CO₂ emission problems instead of more expensive and ineffective materials.



1. INTRODUCTION

Nowadays, great attention is given to the reduction of greenhouse gas emissions caused by the rapid expansion of industrialization and human activities in the natural ecosystem. The effect of greenhouse gases leads to environmental pollution, increases global warming, and affects the balance of the ecosystem.¹ Among them, carbon dioxide is labeled as the main greenhouse gas (GHG) that contributes to global warming through anthropogenic emissions from fossil fuel combustion in power plant generation, transportation, and the industrial sector.^{2,3} Utilization of fossil fuel as the main energy source contributes about 40% of total carbon dioxide emissions, and a 50% increase in carbon dioxide emissions is predicted from fossil fuel-fired power plants alone by 2030.^{4,5} To overcome the major effects of global warming, mitigation of the CO₂ emission is desirable. For this reason, immediate and continuous action should be taken to decrease the CO₂ concentration in the atmosphere. The CO₂ reduction can be done by some options such as reducing the use of fossil fuel, switching to noncarbon-emitting resources, i.e., renewable energy, and permanently capturing and sequestering carbon dioxide (CCS).⁶ However, the utilization of noncarbon-emitting energy resources (i.e., green technologies) still requires significant modifications to the current energy

framework. The great challenges facing these green technologies lie in the difficulty for implementation at an industrial scale, which makes it economically infeasible when compared to fossil fuel-based power plants. This implies that unless green energy alternatives and energy infrastructure for the commercialization and the implementation of these new technologies are attained, the search of new CO₂ emission reduction technologies could be the best alternative to address greenhouse gas effects until the advancement in clean energy technologies reaches commercial stages.⁷

To date, researchers are struggling in searching for an effective strategy to capture carbon dioxide. For instance, liquid solvent absorption, adsorption, membrane separation, and cryogenic distillation are among the developed methods for CO₂ capture.^{8–12} Liquid amine-based solutions such as monoethanolamine (MEA), diethanolamine (DEA), and 2-amino-2-methyl-1-propanol (AMP) have been efficiently

Received: March 14, 2022

Accepted: May 10, 2022

Published: May 25, 2022



applied for CO₂ capture in the industrial fields. However, a liquid amine-based solution to CO₂ capture is highly limited by several disadvantages such as amine degradation, high energy requirement, foaming problems, and equipment corrosion.^{13,14}

On the other hand, a less energy-intensive method, e.g., membrane separation technologies, has been developed to overcome these drawbacks. However, the high cost of membrane separation technologies limits its large-scale application. Recently, solid adsorption technology has received significant attention and is proposed as one of the most promising alternatives for CO₂ capture due to its potential of having a lower cost, less corrosion, and is less energy intensive than the amine scrubbing/membrane method. Among the existing solid adsorbents, the utilization of activated carbon has attracted substantial attention in the field of CO₂ capture because of its robustness, profound stability, feasibility for industrial-scale application, low energy and cost of regeneration, and a highly developed surface area and pore volume.¹⁵

Several researchers have investigated CO₂ capture using commercial activated carbon or modified commercial AC derived from coal, pitch, and other fossil fuel-derived compounds.^{16,17} However, the high cost of current commercial activated carbon and a limited reservoir of fossils highly hinder the economic viability of its wide application. In recent years, the use of various single-substrate-based renewable elemental carbon sources such as Douglas,¹⁵ coffee husk, white wood,¹⁸ bagasse and rice husk,¹⁹ wheat flour,²⁰ peanut shells,²¹ Olive stones,²² coffee residue,²³ etc. have been proposed for preparing activated carbon for CO₂ capture. However, due to limited efficiency and stability, seasonal scarcity of most agricultural wastes, low surface area, and CO₂ adsorption, the efficiency of most single-substrate-based AC is still too low for practical applications. Therefore, it is significantly important to (i) simultaneously convert blends of agricultural wastes into usable products and (ii) build up a multisubstrate-based low-cost AC composite to maximize the CO₂ adsorption capacity, enhance the availability of the substrate in different seasons, improve the stability of the materials, develop a high surface area adsorbent, and enhance the potential of adsorptive separation. To the best of our knowledge, there is no report on preparation of AC from multisubstrate-based agricultural waste for CO₂ capture and modification of the prepared AC with Na₂CO₃.

In this study, we used different multisubstrate agricultural wastes as a precursor to synthesize activated carbon composites for the first time. More briefly, agricultural wastes such as peanut shells (PNS), coffee husks (CH), corn cobs (CC), and banana peels (BP) were used to prepare the multisubstrate AC for the removal of CO₂. The precursors were dried in an oven at 120 °C for 24 h, ground individually to fine powder by a mortar and pestle, and sieved with a 0.25 mm mesh to obtain the particles of uniform size. The sieved biomass powder sample was analyzed for proximate and chemical composition. Finally, the AC composite was prepared by mixing the four biomass powders on the basis of their proximate and chemical compositions. The multisubstrate composition ratio, the effect of different activating agents, and optimization of activated carbon production parameters were considered during the preparation of AC composites. The synthetic procedure is simple, scalable, and inexpensive. The morphology, crystallites, and surface area of the prepared agricultural waste-derived composite AC were examined with SEM, XRD, Raman spectroscopy, and an autosorb IQ

automated gas sorption analyzer. The adsorption capacity of the prepared AC composites as CO₂ adsorbents was investigated using a gas analyzer.

2. EXPERIMENTAL SECTION

2.1. Chemicals and Reagents. Hydrochloric acid (HCl, 37%), potassium iodide (KI, 99%), iodine (I₂, 99.8%), sodium thiosulphate (Na₂S₂O₄, 99%), and starch were purchased from Acros Organics. Sodium carbonate (Na₂CO₃, 98%), sodium hydroxide (NaOH, 98%), potassium hydroxide (KOH), nitric acid (HNO₃, 72%), sulfuric acid (H₂SO₄, 98%), glacial acetic acid (CH₃COOH, 99%), D-glucose (99%), and the anthrone reagent (96%) were purchased from Alfa Aesar. All of the chemicals were used as bought without further purification.

2.2. Collection of Agricultural Waste. All of the agricultural wastes used in this study were collected (15 g each) from the southern nations, nationalities, and people's regions (SNNPR), Ethiopia. The peanut shell (PNS) agricultural waste was collected from Wolaita Zone in SNNPR, while the coffee husk (CH), banana peel (BP), and corn cob (CC) wastes were collected from the markets around Dilla town. The obtained agricultural wastes were washed, dried at 120 °C for 24 h, ground, and sieved to the desired size (less than 250 μm). Then, the sieved biomass powdered sample was analyzed for proximate and chemical composition like cellulose content using standard procedures (see detailed information in the [Supporting Information](#)).

2.3. Preparation of Composite AC from Multisubstrate Agricultural Wastes. On the basis of proximate analysis and chemical composition (i.e., depending on having high cellulose content, volatile matter, and low ash content of the precursor), four biomass powders were mixed up in an optimum ratio. Five different composite ratio substrates such as A (PNS/CH/CC/BP), B (2PNS/CH/CC/BP), C (PNS/2CH/CC/BP), D (PNS/CH/2CC/BP), and E (PNS/CH/CC/2BP) were impregnated with sodium carbonate (one to one ratio, w/w) for 12 h at room temperature. The slurry form of the composite powder was mixed and kept for soaking Na₂CO₃ on its surface. Then, the excess solution was filtered and dried for 8 h in an oven at 110 °C. The dried sample was carbonized in an electric muffle furnace at 400 °C for 90 min. After carbonization, the mixture was removed from the furnace and allowed to cool at room temperature. The pyrolyzed carbon was washed with 5% HCl two to three times, and then washed several times with distilled water until a neutral pH was reached. Afterward, the carbon paste was dried in a drying oven at 110 °C for 24 h, then cooled at room temperature and sieved by 250 μm mesh size. In this study, parameters such as the effect of chemical activating agents, chemical impregnation ratio, impregnation time, carbonization temperature, and carbonization time were studied in depth (see further information in the [Supporting Information](#)).

2.4. Characterization of the AC Composites. The prepared AC composites were characterized by determining the iodine number, X-ray diffraction (XRD), scanning electron microscopy (SEM), Raman spectroscopy, and an autosorb IQ automated gas sorption analyzer. The iodine number is determined following the ASTM D4607-94 method; detailed information is provided in the [Supporting Information](#).²⁴ X-ray diffraction (XRD) patterns were acquired with a D2 phaser XRD-300 W, with measurements taken using Cu Kα radiation at 40 kV and 100 mA. The X-ray patterns were recorded using a linear silicon strip "Lynx Eye" detector from 10 to 70° at a

scan rate of 0.1°/min. The morphology and the composition of the samples in this study were obtained using field-emission scanning electron microscopy (FESEM, JSM 6500F, JEOL) coupled with energy dispersive X-ray analysis (EDS). To enhance the conductivity of the sample, Pt was sputtered on the surface of the samples, and the images were taken at an accelerating voltage of 15 kV. Raman measurements were performed on a ProMaker confocal Raman microscope system as integrated by Protrustech Co., Ltd. A solid-state laser operating at $\lambda = 532$ nm was used as an excitation source with a laser power of 20 mW to circumvent degradation with 10 s exposure times and 15 accumulations. The BET-specific surface area of the AC composites was obtained from N₂ adsorption/desorption data measured at 77.4 K using an autosorb IQ automated gas sorption analyzer. The samples were degassed at 50 °C for 3 h prior to N₂ adsorption. The specific surface area of the sample was calculated using the multiple-point Brunauer–Emmett–Teller (BET) method in the relative pressure range (P/P_0) of 0.05–0.3.

2.5. Adsorption Experiments. A gas analyzer (Figure S1) was used to study the initial and final composition of CO₂ adsorbed on the adsorbents (composite substrate activated carbon). A commercially bought carbon dioxide with a 99.9% purity gas cylinder with a flow rate controller was connected with the clean empty glucose bag tube. Before measurement, the sample was degassed at 120 °C in an oven for 24 h to remove any moisture and CO₂ molecules adsorbed in the pores. After being filled with a given mass of the adsorbate, the adsorption column was connected with a CO₂ source and glucose bag. Then, CO₂ was introduced directly into the system through a constant flow rate. The outlet gas was collected to analyze the gas composition by a gas analyzer (GeoTech gas analyzer UK model). The adsorbed gas volume was measured by an airtight syringe. Consequently, the removal efficiency and adsorption capacity of CO₂ were calculated using eqs 1 and 2, respectively

$$\text{CO}_2 \text{ removal efficiency (\%)} = \left(\frac{C_0 - C_1}{C_0} \right) \times 100 \quad (1)$$

$$\text{CO}_2 \text{ adsorption capacity (wt \%): } q_e = \frac{V_p \times MW \times 100}{V_{\text{molSTP}}} \quad (2)$$

where C_0 and C_1 are the initial and the final CO₂ concentration, respectively, q_e is the adsorption capacity in wt %, V_p is the volumetric adsorption capacity in cm³/g, MW is the adsorbate molecular weight (44.01 g/mol), and V_{molSTP} is the molar volume of a gas at STP (22 414 cm³/mol).

3. RESULTS AND DISCUSSION

3.1. Proximate Analysis and Cellulose Content of Biomass. To examine the suitability of the raw materials as a carbon precursor, we investigated the cellulose content and proximate analysis of the individual agricultural waste substrates. Table 1 shows the cellulose content and proximate analysis of the agricultural wastes (peanut shells, coffee husks, corn cobs, and banana peels). As shown in Table 1, the coffee husk (CH) revealed relatively high cellulose content (53.1%), high volatile matter (80.6%), and low ash content. These results were found to be convenient for the preparation of activated carbon as a starting material. The cellulose content of a corn cob (CC) and a peanut shell was less than that of the

Table 1. Proximate Analysis and Cellulose Content of Agricultural Wastes

precursor	cellulose (%)	ash (%)	moisture (%)	VM (%)	FC
PNS	40.4	4.68	6.40	64.2	22.7
CH	53.1	5.90	7.18	80.6	6.32
CC	42.2	4.32	14.4	68.5	12.8
BP	11.2	9.25	9.41	72.4	8.94

coffee husk but greater than the banana peel's. Moreover, low ash contents of the corn cob and the peanut shell (PNS) precursors indicate that these agricultural waste materials are desirable starting materials of activated carbon. The banana peel (BP) shows high volatile matter but very low cellulose content and relatively greater ash content than the other biomasses. It is known that biomass that contains a high amount of cellulose and low ash content is desirable for the production of activated carbon. Furthermore, the biomass that exhibits high volatile matter is significant as it contributes to the large pore volume of the activated carbon.²⁵

3.2. Multisubstrate Composite Ratio. The multisubstrate agricultural waste-derived composite activated carbon was prepared based on the cellulose content and proximate analysis of the individual agricultural waste materials. That is, we studied the effect of mixing different ratios of the four biomass (i.e., peanut shell, coffee husk, corn cob, and banana peel) based on the cellulose content and proximate analysis. As a result, five multisubstrate-based composites were prepared by mixing different ratios of the aforementioned biomasses (Table 2). The best composite ratio was identified based on the iodine

Table 2. Iodine Value of the Multisubstrate Composite Ratio

code	multisubstrate composite ratio	X/M (mg/g)
A	PNS/CH/CC/BP	348 ± 0.4
B	2PNS/CH/CC/BP	571 ± 0.4
C	PNS/2CH/CC/BP	627 ± 0.3
D	PNS/CH/2CC/BP	514 ± 0.4
E	PNS/CH/CC/2BP	430 ± 0.4

number analysis. Accordingly, the coffee husk doubled composite (PNS/2CH/CC/BP) activated carbon exhibited a higher iodine number compared with the other five types of composite substrate-derived activated carbon. This is because the high cellulose content of coffee husk, corn cob, and peanut shell, as well as a high volatile matters of coffee husk, banana peel, corn cob, and peanut shell, has a great contribution to developing the iodine adsorption capacity of produced composite activated carbon. Consequently, the coffee husk doubled composite substrate was selected as a starting precursor to prepare composite activated carbon.

3.3. Effect of Different Activating Agents. As shown in Table 3, we further studied the effect of different activation agents (chemicals) such as sodium carbonate (Na₂CO₃), sodium hydroxide (NaOH), and potassium hydroxide (KOH) on the iodine value of activated carbon produced from the optimized composite substrate (PNS/2CH/CC/BP). Iodine number analysis is a measure of the micropore content of AC, which is correspondent to the surface area of carbon. A high iodine adsorption capacity indicates the presence of a high surface area and a large amount of micropores in the AC. It has to be noted that the adsorption capacity of an adsorbent is

Table 3. Iodine Value of Activated Carbon Produced by Different Chemical Activations^a

activating agent	IR	IT (h)	CT (°C)	HT (min)	X/M (mg/g)
Na ₂ CO ₃	1:1	12	400	90	627 ± 0.5
NaOH	1:1	12	400	90	564 ± 0.6
KOH	1:1	12	400	90	597 ± 0.9

^aIR—impregnation ratio, IT—impregnation time, CT—carbonization temperature, HT—holding time, and X/M—iodine number.

directly proportional to the surface area and micropore content.²⁶ Compared with the other activating agent, the composite AC (PNS/2CH/CC/BP) activated with sodium carbonate activation showed a relatively higher iodine number (627 mg/g). As clearly shown in Table S1, a significance difference ($p \leq 0.05$) in the mean iodine number value between the composite activated carbon activated with Na₂CO₃, NaOH, and KOH was observed at a 95% confidence interval. The higher iodine number value using Na₂CO₃ might be caused by its reaction with carbon, creating new pores or enlarging existing ones than the other chemicals. Iodine number adsorption indicates that sodium carbonate is the best activating agent among the other activating agents tested.

3.4. Optimum Activated Carbon Production Parameters. **3.4.1. Effect of the Chemical Impregnation Ratio and Impregnation Time.** To gain insight into the influence of the chemical to substrate impregnation ratio on adsorption properties of the composite, samples were prepared with different impregnation ratios of sodium carbonate (Figure 1a and Table S2). As shown in Figure 1a and Table S2, the iodine number of activated carbon increased from 700 to 721 mg/g with increasing the impregnation ratio of chemical to the composite substrate (w/w) from 0.20 to 0.25. However, the corresponding iodine number of the produced activated carbon decreases with increasing the impregnation ratio beyond 0.25. The reduction in adsorption property at a higher impregnation ratio might be due to the decrease in the number of micropores on the activated carbon or accumulation of an excessive activating agent on the activated carbon surface or the effect of pore widening and destruction of pore walls between neighboring pores.²⁷ We further studied the effect of impregnation time on the adsorption property of the as-prepared composite activated carbon. Figure 1b and Table S3 show the changes in the iodine number of activated carbon produced from a multisubstrate composite as a function of impregnation time. As shown in Figure 1b, it is clear that impregnation time significantly affects the iodine adsorption

property of activated carbon. Increasing the activation time from 6 to 24 h increases the iodine value from 654 to 741 mg/g (see Figure 1b and Table S3), which might be due to the volatilization of organic matter from precursors. But the iodine number decreases rapidly when the activation is carried out for a longer time. That is, under extended activation time, the microporous structure of the produced activated carbon deteriorated and turned into mesopores or macropores.²⁸

3.4.2. Effect of Carbonization Temperature and Time. We also examined the influence of carbonization temperature and time on the production of activated carbon from agricultural wastes (Figure 2 and Tables S4 and S5). At the same impregnation ratio (0.25) and impregnation time (24 h), the as-prepared composite activated carbon obtained at a carbonization temperature of 450 °C revealed the highest iodine number of 774 mg/g (Figure 2a and Table S4). This value is greater than the corresponding value reported before (765 mg/g).²⁹ It is noted that the iodine adsorption number is an indication of the total surface area of the activated carbon and a measure of the activity level.³⁰ That means the adsorbent with a higher iodine number could show higher adsorption capacity at optimum production parameters. The porous character of the as-prepared composite activated carbon was further investigated by optimizing the carbonization time between 30 and 150 min (Figure 2b and Table S5). As shown in Figure 2b, the highest iodine number, 774 mg/g, was attained when the impregnated composite substrate was carbonized for 90 min. Further increasing the carbonization time decreases the iodine number. The iodine number obtained in this study is above 700 mg/g, suggesting the presence of good porosity and meeting the commercial usability criteria.³¹ The iodine number is a measure of the activity level or micropore content of the activated carbon, frequently reported in mg/g (with a typical range of 500–1200 mg/g). It is equivalent to the surface area of activated carbon between 900 and 1100 m²/g.²⁶ The iodine number of the sodium carbonate-activated composite carbon (SC-CAC) was compared with (i) sodium hydroxide and potassium hydroxide activated composite carbon (SH-CAC and PH-CAC, respectively) and sodium carbonate-activated coffee-husk-only-derived AC (SC-CHAC) at the same optimal conditions and (ii) with other adsorbents reported before (Table S6). The adsorption capacity of the SC-CAC is unprecedented among the prepared adsorbents and adsorbents reported before. Motivated by the above findings, the percentage yield of the AC in the composite was also examined. The minimum percentage yield was recorded when the activated carbon

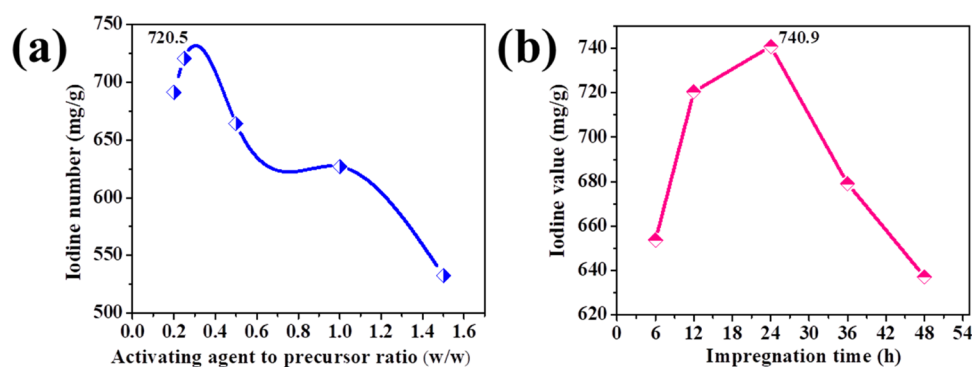


Figure 1. Effect of (a) chemical activation to precursor ratio and (b) impregnation time.

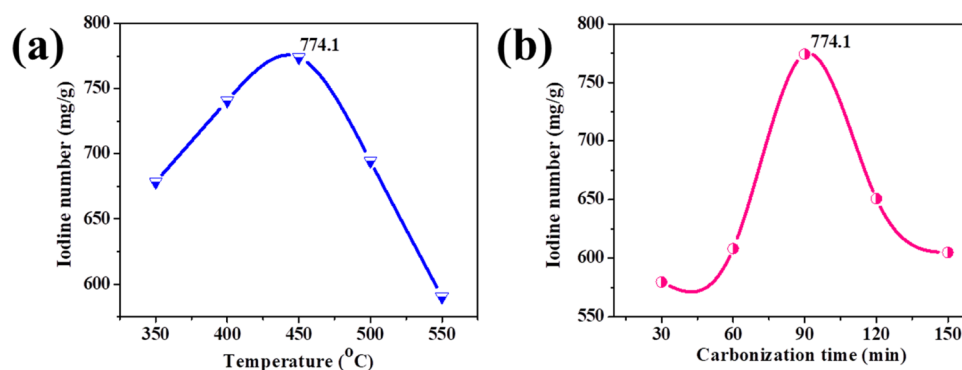


Figure 2. Effect of (a) carbonization temperature and (b) carbonization time.

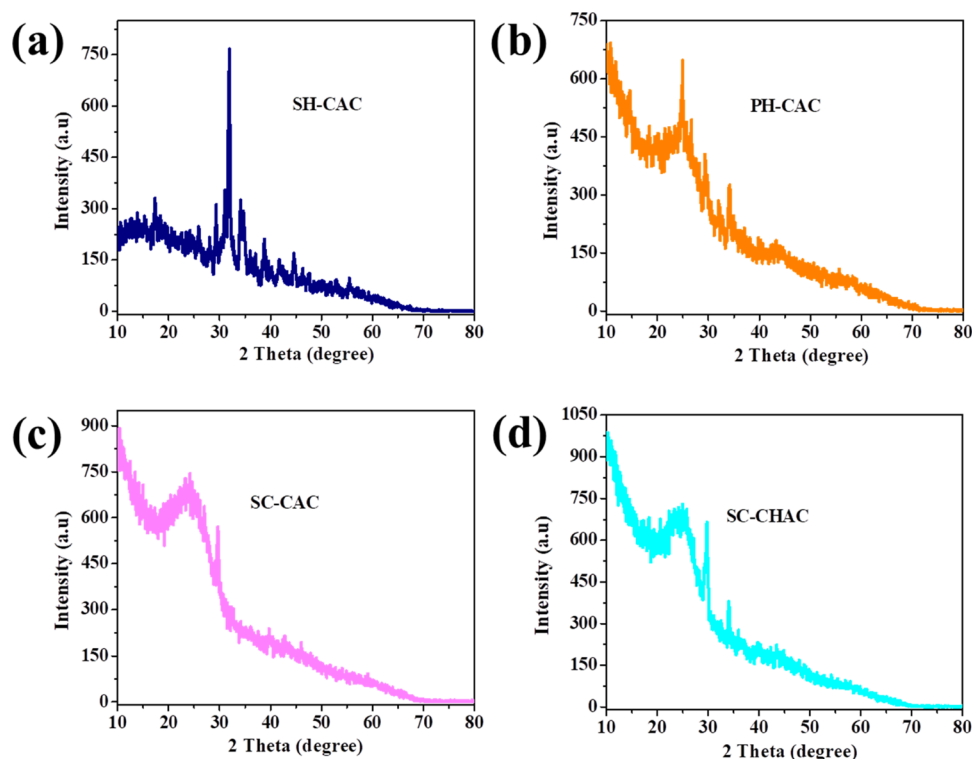


Figure 3. XRD patterns of SH-CAC (a), PH-CAC (b), SC-CAC (c), and SC-CHAC (d).

composite was not chemically activated (Table S7). However, the percentage yield increases from 58.1 to 92.3% when the sodium carbonate content increases from 0.2 to 0.25. The maximum percentage yield (92.3%) was achieved by the AC-0.25 sample, indicating enhanced pore opening and widening caused by the activating agent at an optimal concentration. A decrease in the percentage yield was observed when the concentration of Na_2CO_3 increased beyond 0.25.

3.5. Crystallinity and Morphology Studies. The crystalline properties of the as-prepared composite-activated carbon (CAC) activated with various activating agents were characterized by X-ray diffraction (XRD). Figure 3 shows the XRD patterns of CAC and coffee husk-derived activated carbon (CHAC) activated with sodium hydroxide, potassium hydroxide, and sodium carbonate (i.e., SH-CAC, PH-CAC, SC-CAC, and SC-CHAC). The sodium hydroxide activated composite (SH-CAC) sample exhibits a very sharp peak at about 32.05° , indicating a more crystal structure of the carbon material and a less amorphous structure compared with the

other three activated carbon materials (Figure 3). As clearly observed in Figure 3a–d, the nature of the XRD pattern is quite different as we changed the activating agent from sodium hydroxide to potassium hydroxide or sodium carbonate. The XRD pattern of CAC activated with potassium hydroxide (Figure 3b) and sodium carbonate (Figure 3c) exhibits the absence of the peak at 32.05° and the presence of a broad peak at about 24.94 and 24.43° , respectively, and a highly diminished diffraction peak at about 43° . These patterns are known to be characteristic of the disordered graphite-like structure of amorphous carbon, which exhibits a superior advantage for advanced solid–gas adsorption due to its porous nature.³² Although the peak is slightly narrower in nature, the AC prepared from coffee husk only (Figure 3d) revealed the same pattern as the CAC activated with the same reagent. The finding in this study is in good agreement with previously reported AC prepared from jute fibers.²⁷ The calculated grain size (i.e., using the Scherrer equation) was less than 2 nm, indicating a microporous characteristic nature of the prepared

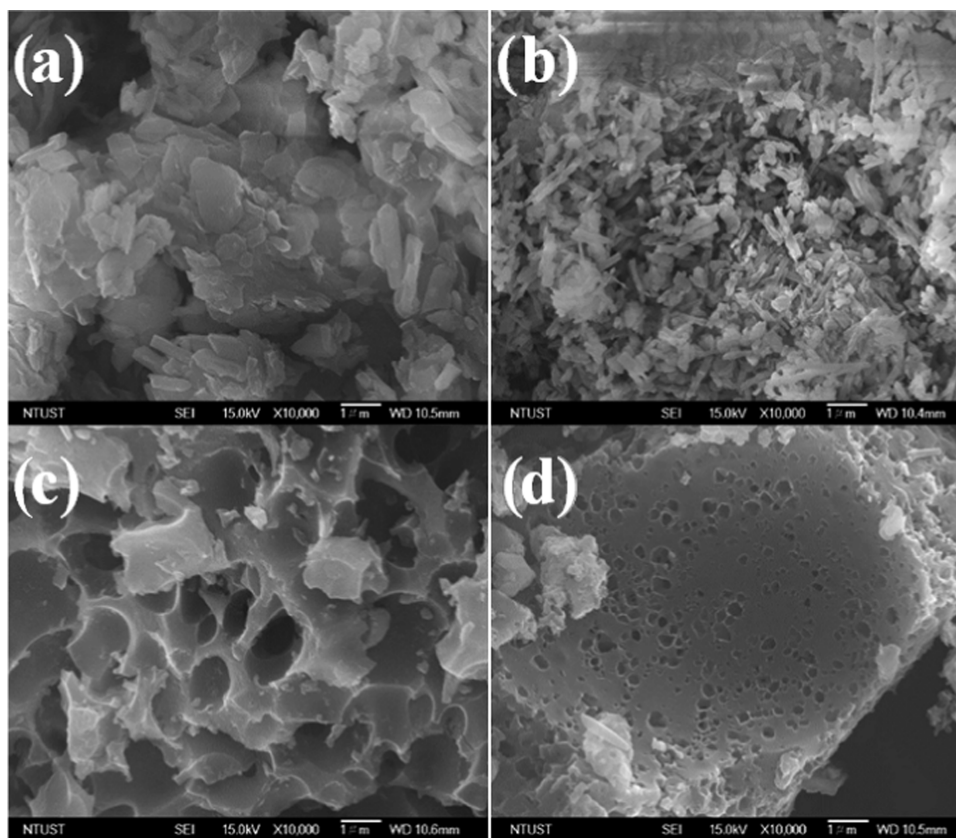


Figure 4. SEM images of (a) SH-CAC, (b) PH-CAC, (c) SC-CAC, and (d) SC-CHAC.

carbon materials. This agrees well with the iodine adsorption number analysis. The graphitic nature of the carbon material changes a lot with the change in the activating agent (e.g., as shown in Table S8, it decreases from SH-CAC to SC-CAC) due to an increase in the porosity of the produced activated carbon.³¹ This supports that SC-CAC and SC-CHAC were found to be more amorphous in nature than PH-CAC and SH-CAC.

We investigated the presence or absence of porosity on the synthesized composite activated carbon derived from multi-substrate agricultural wastes and coffee-husk-only-based activated carbons, namely, SH-CAC, PH-CAC, SC-CAC, and SC-CHAC, using a field-emission scanning electron microscope (Figure 4). As shown in Figure 4a, the SEM image of SH-CAC revealed no well-developed pores or surface heterogeneity compared with the other three produced activated carbon. The SEM images for PH-CAC and SC-CAC in Figure 4b,c, respectively, display more or less heterogeneous surface morphology with a porous structure in various sizes. However, the SC-CAC shows more surface heterogeneity, huge cavities, and well-developed pores with a variety of randomly dispersed pore sizes. These well-developed pores, surface heterogeneity, and the cavities of activated carbon were found to be suitable for gas-phase adsorption applications. The activated carbon derived from the coffee-husk-only substrate (Figure 4d) revealed a smoother surface with some pore openings at the same magnification. The growth of the porosity on the exterior of the activated carbon structure is caused by the removal of inorganic materials that tend to clog the pores. Furthermore, the development of porosity on the activated carbon after the chemical activation

indicates that there is a good opportunity for the CO₂ molecules to be trapped and adsorbed inside these pores.³³

We further examined the elemental composition of the agricultural waste-derived composites and coffee-husk-only-activated carbons (SH-CAC, PH-CAC, SC-CAC, and SC-CHAC) using energy dispersive spectroscopy (EDS). Figure 5 shows the SEM-EDS analysis of agricultural waste-derived composite and single-substrate-activated carbons such as SH-CAC, PH-CAC, SC-CAC, and SC-CHAC. These materials mainly contain carbon and oxygen in different proportions. The percentage weight of carbon in the SH-CAC, PH-CAC, SC-CAC, and SC-CHAC is 34.83, 67.20, 85.33, and 79.16, respectively. The SC-CAC sample exhibits a higher percentage weight of carbon (85.33%) than the other samples, indicating the presence of abundant micropores. This result supports that SC-CAC has the highest pore volume or heterogeneous surface compared with the others. The result from the SEM-EDS analysis is in good agreement with our XRD measurements.

3.6. Surface Area and Raman Studies. Inspired by the aforementioned characterizations, the surface areas and pore volumes of the agricultural waste-derived composites and coffee-husk-only-activated carbons were investigated using N₂ adsorption–desorption isotherms (Figure 6a). According to the International Union of Pure and Applied Chemistry (IUPAC) classification, the N₂ adsorption–desorption isotherms of all of the samples were assigned to type IV isotherm with a nearly H1 hysteresis loop, indicating the presence of mesopores resulting from the effect of the activating agent. It is also observed that the hysteresis loop shifts toward $P/P_0 = 1.0$, indicating the presence of macropores, particularly by SC-CAC and SC-CHAC samples. Furthermore, the absence of a plateau at high relative pressure P/P_0 in the adsorption isotherm

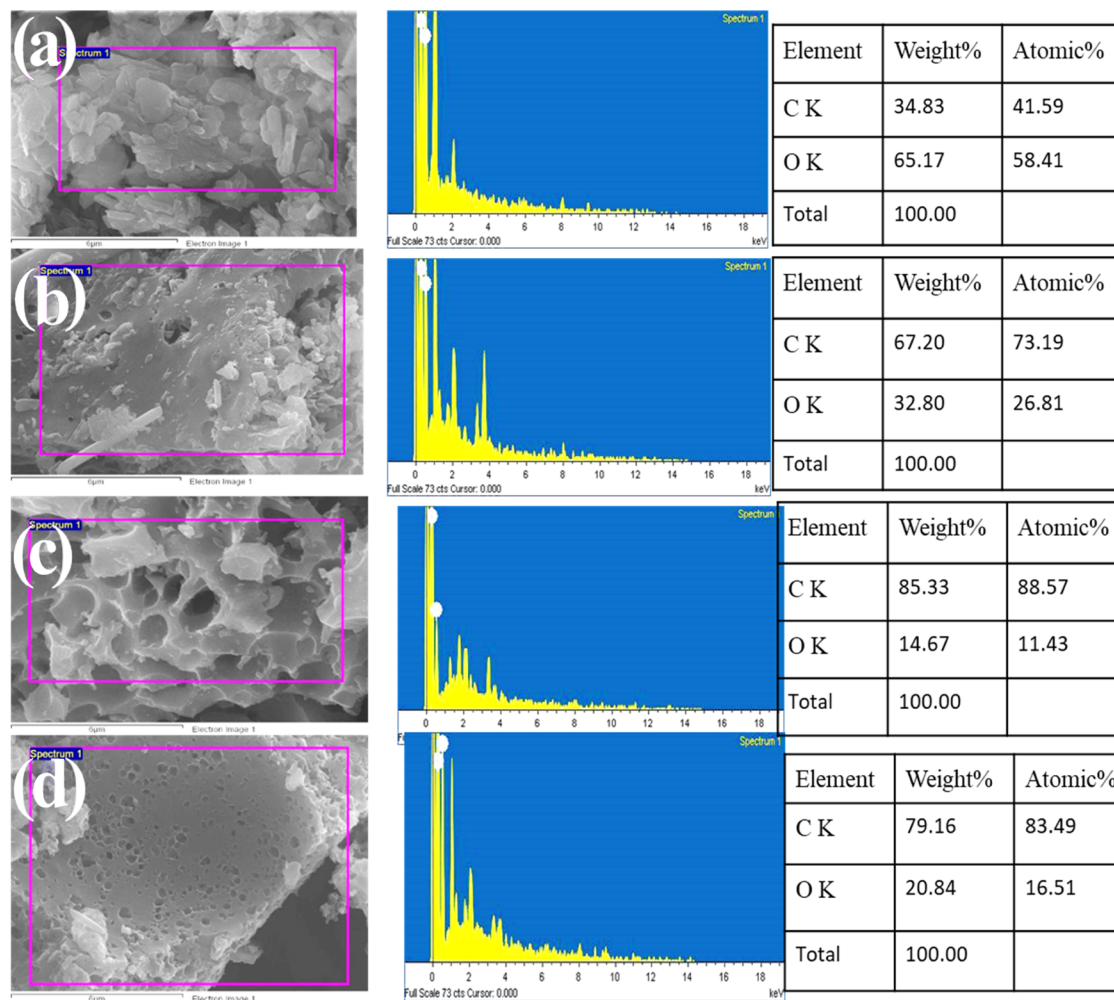


Figure 5. EDX analysis of (a) SH-CAC, (b) PH-CAC, (c) SC-CAC, and (d) SC-CHAC.

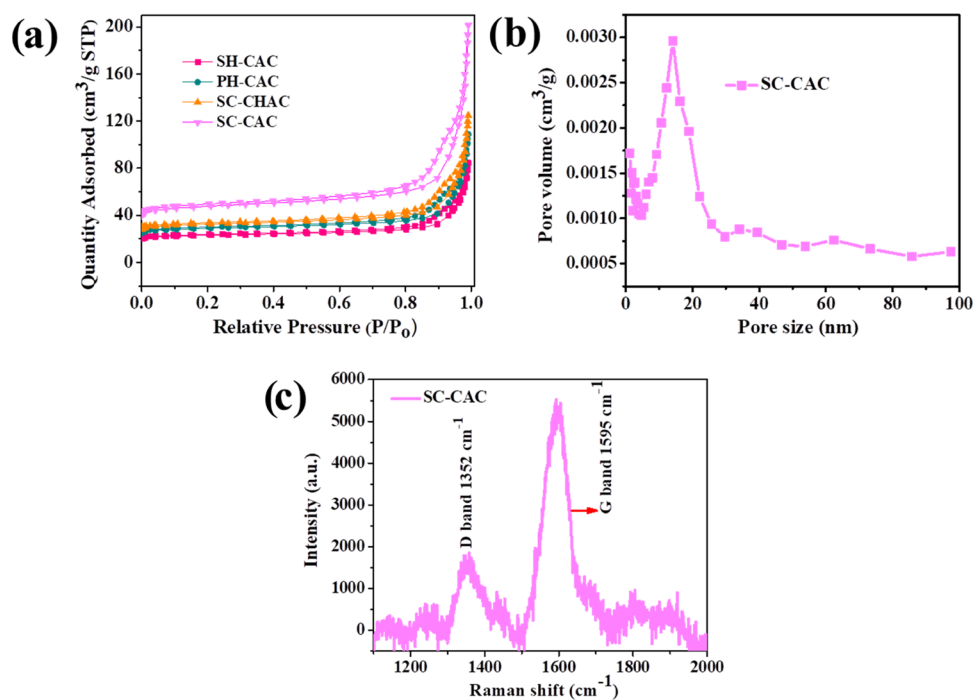


Figure 6. (a) N_2 adsorption–desorption isotherms of all samples, (b) BJH pore size distribution, and (c) Raman spectra of the SC-CAC sample.

indicates the coexistence of macropores (>50 nm) inside the prepared samples.³⁴ The BET surface areas of the as-prepared composite activated carbon from multisubstrate agricultural wastes (namely SC-CAC, SH-CAC, and PH-CAC) and AC from coffee-husk-only waste (i.e., SC-CHAC) were found to be 1239, 275, 426, and 931 m²/g, respectively. The sodium carbonate-activated agricultural waste-derived composites (SC-CAC) provided the maximum surface area, which lies within the acceptable range of commercial activated carbon (500–1500 m²/g).³⁵ This indicates the maximum removal of inorganic materials causing structural heterogeneity, which is convenient for advanced solid–gas adsorption behavior. The reduced surface area via using hydroxide-based chemical might be due to its insufficient activating role toward removing inorganic material from the mother substrate. Moreover, the pore size distribution and pore volume of all of the samples were examined using the Barrett–Joyner–Halenda (BJH) method (Table S9). Among all of the prepared samples, the SC-CAC sample demonstrated the highest surface area and pore volume (0.097 cm³/g), further indicating the presence of larger mesopores and macropores (Figure 6b). The information obtained from the pore size distributions and adsorption isotherms are in good agreement with the SEM images. The BET surface area and total pore volume of the produced activated carbon materials were also compared with other AC-based adsorbents (Table S10). Except for the surface area of pumpkin seed shell-based AC, the multisubstrate agricultural waste-derived activated carbon (SC-CAC) exhibited an extremely higher surface area and total pore volume as compared with AC derived from different biomasses. Thus, the findings in this study are encouraging to produce activated carbon with a high surface area, pore volume, and high adsorption capacity.

We further studied the crystallographic disorder in carbons materials using Raman spectroscopy. As shown in Figure 6c, the Raman spectra of the agricultural waste-derived composite activated carbon using sodium carbonate (SC-CAC) revealed two major peaks, namely D and G peaks. The G and D peaks are assigned to the in-plane stretching motion between sp² carbon atoms and the disordered band originating in structural defects, edge effects, and dangling sp² carbon bonds that break the symmetry.³⁶ The D and G peak positions are centered at 1352 and 1595 cm⁻¹ for the SC-CAC sample, respectively. The intensity of the G peak is higher than that of the D peak for produced SC-CAC. The D and G peak positions and their intensity ratios are widely used for the identification of the type and characterization of the structure of amorphous carbons. The peak intensity ratio of D and G bands (I_D/I_G) for SC-CAC was found to be 0.331. The smaller peak intensity ratio I_D/I_G corresponds to a higher degree of AC graphitization and the greater ratio corresponds to a higher degree of AC amorphous.¹⁶

3.7. Adsorption Experiment. Commercially bought carbon dioxide was taken for the adsorptions experiments. The height of the column for the adsorption experiments was 8 and 2 cm in diameter, with an inlet at the bottom and an outlet at the top of the column. A total of 1 g of produced activated carbon powder was filled into a column, and commercial CO₂ was passed through the inlet at a constant flow rate of 5 LPH (liter per hour). The outlet gas was collected in the gas bags (glucose bag) with a flow controller in the bag. Then, the collected gas composition was analyzed by a gas analyzer. With the help of the gas analyzer and an airtight syringe, the

composition of CO₂ adsorbed in the produced activated carbon was calculated. The percentage composition of the carbon dioxide before adsorption (initial) was 99.9%. The percentage composition of carbon dioxide after adsorption was reduced to 3.80% within 3 min of a constant flow rate and at STP. The removal efficiency was calculated using the formula

$$\begin{aligned}\text{CO}_2 \text{ removal efficiency (\%)} &= \frac{(99.9 - 3.8)}{99.9} \times 100 \\ &= 96.2\%\end{aligned}$$

The collected CO₂ gas volume was measured by an airtight syringe before and after adsorption took place at different residence times with 1 g of prepared composite activated carbon. The consumed or considered as adsorbed CO₂ volume was obtained by taking the difference between the initial and final volume of carbon dioxide gas (Figure S2). As shown in Figure S2, the carbon dioxide adsorption capacity of the produced activated carbon increases from 1 to 3 min, but after 3 min, it shows a slight decrease. Thus, the maximum adsorption capacity of 8.86 wt % was achieved at a 3 min residence time with 1 g of the agricultural waste multisubstrate composite substrate (PNS/2CH/CC/BP) activated carbon (SC-CAC). Accordingly, the produced multisubstrate composite activated carbon of the present study showed a promising CO₂ adsorption capacity than the single-biomass-activated carbon.

4. CONCLUSIONS

To summarize, we have successfully prepared a composite activated carbon (CAC) via tuning the ratio of four agricultural wastes (i.e., peanut shell, coffee husk, corn cob, and banana peel) using the cellulose content and proximate analysis values as a basis. The as-synthesized composite activated carbon was investigated for the removal of CO₂ by adsorption. The CAC obtained by doubling the coffee husk (PNS/2CH/CC/BP) exhibited a higher iodine number compared with the other four types of composite substrate-derived activated carbon. The Na₂CO₃-activated CAC showed a higher surface area and valuable textural properties for CO₂ adsorption compared with the KOH- and NaOH-activated carbon materials. An optimal carbonization temperature (450 °C), carbonization time (24 h), Na₂CO₃/composite impregnation ratio (0.25, w/w), and time (90 min) were identified for pyrolysis of the noncarbon element, revealing immense micropores, which can be easily accessible by the gas molecules. The CACs were characterized by X-ray diffraction (XRD), scanning electron microscopy (SEM), energy dispersive spectroscopy (EDS), Raman spectroscopy, N₂ adsorption–desorption isotherm, and iodine number analysis that shows that the material is capable to adsorb the adsorbate. The CAC obtained at optimal conditions exhibited the highest CO₂ removal efficiency and adsorption capacity of 96.2% and 8.86 wt %, respectively, compared with the single-biomass-derived activated carbon. The enhanced CO₂ adsorption performance is due to the large surface area, a considerable extent of mesopores, and a suitable pore width of the prepared CAC. The adsorbent in this study reveals a promising strategy for mitigating the CO₂ emission problems instead of more expensive and ineffective materials.

■ ASSOCIATED CONTENT

SI Supporting Information

The Supporting Information is available free of charge at <https://pubs.acs.org/doi/10.1021/acsomega.2c01528>.

Chemicals and reagents, apparatus and instruments, cellulose content and proximate analysis of agricultural wastes, preparation of the multisubstrate AC composite, optimization of activated carbon production parameters, iodine test, adsorption experimental design, one-way ANOVA test, percentage yield of the as-prepared composite activated carbon, grain size of agricultural waste-derived activated carbons, BET information for the prepared composite AC, comparison of the surface area and total pore volume of various activated carbons, and carbon dioxide adsorption capacity at different residence times (PDF)

■ AUTHOR INFORMATION

Corresponding Author

Amare Aregahegn Dubale – Department of Chemistry, College of Natural and Computational Science, Energy and Environment Research Center, Dilla University, Dilla, Ethiopia; orcid.org/0000-0002-7674-5709; Email: amare2122@gmail.com

Authors

Mardikios Maja Bade – Department of Chemistry, College of Natural and Computational Science, Energy and Environment Research Center, Dilla University, Dilla, Ethiopia

Dawit Firemichael Bebizuh – Department of Chemistry, College of Natural and Computational Science, Energy and Environment Research Center, Dilla University, Dilla, Ethiopia

Minaleshewa Atlabachew – Department of Chemistry, College of Science, Bahir Dar University, Bahir Dar 6000, Ethiopia

Complete contact information is available at:

<https://pubs.acs.org/doi/10.1021/acsomega.2c01528>

Notes

The authors declare no competing financial interest.

■ ACKNOWLEDGMENTS

The authors would like to gratefully acknowledge the Department of Chemistry and Energy and Environment Research Center at Dilla University for financial support and provision of laboratory facilities. The authors are also very thankful to Dr. Daneil Manaye and Dr. Alemayehu Dubale for their heartfelt cooperations in data measurements.

■ REFERENCES

- (1) Liu, Y.; Ye, Q.; Shen, M.; Shi, J.; Chen, J.; Pan, H.; Shi, Y. Carbon dioxide capture by functionalized solid amine sorbents with simulated flue gas conditions. *Environ. Sci. Technol.* **2011**, *45*, 5710–5716.
- (2) Zhang, C.; Song, W.; Sun, G.; Xie, L.; Wang, J.; Li, K.; Sun, C.; Liu, H.; Snape, C. E.; Drage, T. CO₂ Capture with Activated Carbon Grafted by Nitrogenous Functional Groups. *Energy Fuels* **2013**, *27*, 4818–4823.
- (3) Darunte, L. A.; Oetomo, A. D.; Walton, K. S.; Sholl, D. S.; Jones, C. W. Direct Air Capture of CO₂ Using Amine Functionalized MIL-101(Cr). *ACS Sustainable Chem. Eng.* **2016**, *4*, 5761–5768.
- (4) Hauchhum, L.; Mahanta, P. Carbon dioxide adsorption on zeolites and activated carbon by pressure swing adsorption in a fixed bed. *Int. J. Energy Environ. Eng.* **2014**, *5*, 349–356.
- (5) Wickramaratne, N. P.; Jaroniec, M. Activated carbon spheres for CO₂ adsorption. *ACS Appl. Mater. Interfaces* **2013**, *5*, 1849–1855.
- (6) Leung, D.Y.C.; Caramanna, G.; Maroto-Valer, M. M. An overview of current status of carbon dioxide capture and storage techniques. *Renewable Sustainable Energy Rev.* **2014**, *39*, 426–443.
- (7) Sailee, D. S.; Kavita, K. Adsorption of Carbon Dioxide on Adsorbents Synthesized by Microwave Technique. *J. Chem. Eng. Process. Technol.* **2015**, *6*, No. 1000259.
- (8) Chen, Y.-H.; Lu, D. L. Amine modification on kaolinites to enhance CO₂ adsorption. *J. Colloid Interface Sci.* **2014**, *436*, 47–51.
- (9) Bredesen, R.; Jordal, K.; Bolland, O. High-temperature membranes in power generation with CO₂ capture. *Chem. Eng. Process.* **2004**, *43*, 1129–1158.
- (10) Plaza, M. G.; Pevida, C.; Arenillas, A.; Rubiera, F.; Pis, J. J. CO₂ capture by adsorption with nitrogen enriched carbons. *Fuel* **2007**, *86*, 2204–2212.
- (11) Song, H.-J.; Lee, S.; Maken, S.; Park, J.-J.; Park, J.-W. Solubilities of carbon dioxide in aqueous solutions of sodium glycinate. *Fluid Phase Equilib.* **2006**, *246*, 1–5.
- (12) Bertelle, S.; Vallières, C.; Roizard, D.; Fravre, E. Design, synthesis and characterization of mixed matrix material for CO₂ capture. *Desalination* **2006**, *200*, 456–458.
- (13) D'Alessandro, D. M.; Smit, B.; Long, J. R. Carbon dioxide capture: prospects for new materials. *Angew. Chem., Int. Ed.* **2010**, *49*, 6058–6082.
- (14) Rashidi, N. A.; Yusup, S.; Hameed, B. H. Kinetic studies on carbon dioxide capture using lignocellulose based activated carbon. *Energy* **2013**, *61*, 440–446.
- (15) Yadavalli, G.; Lei, H.; Lei, Y. W.; Zhu, L.; Zhang, X.; Liu, Y.; Yan, D. Carbon dioxide capture using ammonium sulfate surface modified activated biomass carbon. *Biomass Bioenergy* **2017**, *98*, 53–60.
- (16) Sreńscek-Nazzal, J.; Narkiewicz, U.; Morawski, A. W.; Wróbel, R.; Geskiewicz-Puchalska, A.; Michalkiewicz, B. Modification of Commercial Activated Carbons for CO₂ Adsorption. *Acta Phys. Pol. A* **2016**, *129*, 394–401.
- (17) Siriwardane, R. V.; Shen, M.-S.; Fisher, E. P.; Poston, J. A. Adsorption of CO₂ on Molecular Sieves and Activated Carbon. *Energy Fuels* **2001**, *15*, 279–284.
- (18) Shahkarami, S.; Azargohar, R.; Dalai, A. K.; Soltan, J. Breakthrough CO₂ adsorption in bio-based activated carbons. *J. Environ. Sci.* **2015**, *34*, 68–76.
- (19) Boonpoke, A.; Boonpoke, A.; Chiarakorn, S.; Laosiripojana, N.; Towprayoon, S.; Chidthaisong, A. Synthesis of Activated Carbon and MCM-41 from Bagasse and Rice Husk and their Carbon Dioxide Adsorption Capacity. *J. Sustainable Energy Environ.* **2011**, *2*, 77–81.
- (20) Hong, S.-M.; Jang, E.; Dysart, A. D.; Pol, V. G.; Lee, K. B. CO₂ Capture in the Sustainable Wheat-Derived Activated Microporous Carbon Compartments. *Sci. Rep.* **2016**, *6*, No. 34590.
- (21) Lewicka, K. Activated carbons prepared from hazelnut shells, walnut shells and peanut shells for high CO₂ adsorption. *Pol. J. Chem. Technol.* **2017**, *19*, 38–43.
- (22) Moussa, M.; Badera, N.; Querejeta, N.; Durán, I.; Pevida, C.; Ouederni, A. Toward sustainable hydrogen storage and carbon dioxide capture in post-combustion conditions. *J. Environ. Chem. Eng.* **2017**, *5*, 1628–1637.
- (23) Lamine, S. M.; Ridha, C.; Mahfound, H.-M.; Mouad, C.; Lotfi, B.; Al-Dujaili, A. H. Chemical activation of an Activated carbon Prepared from coffee residue. *Energy Procedia* **2014**, *50*, 393–400.
- (24) *Standard Test Method for Determination of Iodine Number of Activated Carbon*; ASTM International: West Conshohocken, PA, 2006.
- (25) Rashidi, N. A.; Yusup, S.; Borhan, A. Development of Novel Low-Cost Activated Carbon for Carbon Dioxide Capture. *Int. J. Chem. Eng. Appl.* **2014**, *5*, 90–94.

(26) Windle, C. D.; Pastor, E.; Reynal, A.; Whitwood, A. C.; Vaynze, Y.; Durrant, J. R.; Perutz, R. N.; Reisner, E. Improving the photocatalytic reduction of CO₂ to CO through immobilisation of a molecular Re catalyst on TiO₂. *Chem. – Eur. J.* **2015**, *21*, 3746–3754.

(27) Ramesh, T.; Rajalakshmi, N.; Dhathathreyan, K. S. Synthesis and characterization of activated carbon from jute fibers for hydrogen storage. *Renewable Energy Environ. Sustainability* **2017**, *2*, No. 4.

(28) Soleimani, M.; Kaghazchi, T. Low-Cost Adsorbents from Agricultural By-Products Impregnated with Phosphoric Acid. *Adv. Chem. Eng. Res.* **2014**, *3*, 34–41.

(29) Mussatto, S. I.; Fernandes, M.; Rocha, G. J. M.; Órfão, J. J. M.; Teixeira, J. A.; Roberto, I. C. Production, characterization and application of activated carbon from brewer's spent grain lignin. *Bioresour. Technol.* **2010**, *101*, 2450–2457.

(30) Rosas, J. M.; Bedia, J.; Rodríguez-Mirasol, J.; Cordero, T. HEMP-derived activated carbon fibers by chemical activation with phosphoric acid. *Fuel* **2009**, *88*, 19–26.

(31) Jadhav, A. S.; Mohanraj, G. T. Synthesis and characterization of chemically activated carbon derived from arecanut shell. *Carbon – Sci. Technol.* **2016**, *8*, 32–39.

(32) Das, D.; Samal, D. P.; Meikap, B. C. Preparation of Activated Carbon from Green Coconut Shell and its Characterization. *J. Chem. Eng. Process. Technol.* **2015**, *06*, No. 1000248.

(33) Rashidi, N. A.; Yusup, S.; Hameed, B. H. Kinetic studies on carbon dioxide capture using lignocellulosic based activated carbon. *Energy* **2013**, *61*, 440–446.

(34) Dubale, A. A.; Zheng, Y.; Wang, H.; Hgbner, R.; Li, Y.; Yang, J.; Zhang, J.; Sethi, N. K.; He, L.; Zheng, Z.; Liu, W. High-Performance Bismuth-Doped Nickel Aerogel Electrocatalyst for the Methanol Oxidation Reaction. *Angew. Chem., Int. Ed.* **2020**, *59*, 13891–13899.

(35) Hidayu, A. R. Impregnated Palm Kernel Shell Activated Carbon for CO₂ Adsorption by Pressure Swing Adsorption. *Indian J. Sci. Technol.* **2017**, *10*, 1–6.

(36) Dubale, A. A.; Su, W.-N.; Tamirat, A. G.; Pan, C.-J.; Aragaw, B. A.; Chen, H.-M.; Chen, C.-H.; Hwang, B. J. The synergetic effect of graphene on Cu₂O nanowire arrays as a highly efficient hydrogen evolution photocathode in water splitting. *J. Mater. Chem. A* **2014**, *2*, 18383–18397.